2020

In Vitro Assessment of Dynamic Guidance in Endodontic Microsurgical Osteotomy & Root-End Resection

Bradley Lawrence Sleeth
Medical University of South Carolina

In Vitro Assessment of Dynamic Guidance in
Endodontic Microsurgical Osteotomy & Root-End Resection

Bradley Lawrence Sleeth

A thesis submitted to the faculty of
the Medical University of South Carolina
in partial fulfillment of the requirements for the
degree of Master of Science in Dentistry
in the College of Dental Medicine

Department of Oral Rehabilitation

Division of Endodontics

2020

Approved by:

Chairman, Advisory Committee

Approved on July 27, 2020

T. R

Theodore D. Ravenel

Zachary Evans

Robert P. Bethea

Table of Contents

List of Tables

List of Figures

BRADLEY LAWRENCE SLEETH, D.M.D. In Vitro Assessment of Dynamic Guidance in Endodontic Microsurgical Osteotomy & Root-End Resection. (Under the direction of THEODORE RAVENEL, D.M.D.)

Abstract

Introduction: Dynamic guidance is a technology that uses CBCT images and an array of cameras & sensors to guide the operator's dental handpiece along a pre-determined path in real-time. It has been used in implant surgery, non-surgical endodontics, as well as in a few reported clinical cases of endodontic microsurgery to improve the accuracy of these procedures. However, no study has been published which quantitatively evaluates its ability to improve accuracy and reduce osteotomy size in endodontic microsurgery. Therefore, the aim of this in-vitro study was to compare dynamically guided endodontic microsurgery to freehand surgery in terms of osteotomy window, osteotomy volume, apical bevel, apical resection length and depth of osteotomy past the target root.

Materials and Methods: Thirty-six human mandibular posterior teeth were cast into stone models containing three teeth each (one premolar, two molars), and those models were subsequently divided equally into freehand and guided groups. In the freehand group, an experienced operator performed osteotomies and root-end resections. In the guided group, the X-Guide System was used to assist in the execution of similar osteotomies and resections. Post-operative CBCT images were taken of both groups and the aforementioned parameters were evaluated using software native to the imaging system.

Results: Significant differences were found between the freehand and guided groups in terms of osteotomy window area, osteotomy volume, depth of osteotomy past the target root and amount of resection. Most notably, the window area in the guided group ($15.7mm^2 \pm 3.85$) was significantly ($p<0.05$) smaller than in the freehand group ($37.6mm^2 \pm 5.02$), and the osteotomy volume in the guided group ($0.111cm^3 \pm 0.04$) was significantly ($p<0.05$) smaller than in the freehand group ($0.226cm^3 \pm 0.05$).

Conclusions: The results of this study show that implementing dynamic guidance in endodontic microsurgery has the potential to significantly reduce the osteotomy window area and osteotomy volume as compared to freehand surgery, which subsequently can result in improved healing. It can also ensure that critical structures such as adjacent non-target roots and the mandibular canal are avoided while attempting to locate the target root.

Introduction

Endodontic microsurgery (EMS) has become a critical tool for endodontists to provide the best possible care for their patients (Kim and Kratchman 2006). Indications for EMS include treating teeth with long posts, irretrievable broken files, non-negotiable ledges, canal transportation or blockages, teeth with newly delivered fixed restorations, or teeth in which a biopsy is needed (Hargreaves 2016). While traditional surgical techniques resulted in low success rates of approximately 59%, the implementation of technologies such as the dental operating microscope, ultrasonics & bioceramics in modern endodontic microsurgery has shown significantly improved success rates of up to 94% (Setzer, Shah et al. 2010). The improvement of success rates because of the implementation of new technology has made surgical approaches to treatment much more mainstream. It also begs the question as to which future technologies could continue to provide increased chances of success.

There are myriad factors associated with the success and failure of periapical surgery. In a prospective study including 584 teeth, Song et al. found that tooth type and arch was significantly related to outcome, with mandibular anterior and posterior teeth having lower success rates compared to maxillary anterior teeth (Song, Kim et al. 2013). They concluded that the reduced success in some teeth could be ascribed to limited access hampering the necessary precision of the surgical access.

Likely related to the difficult access and reduced precision discussed by Song, other studies have shown more specifically that osteotomy size affects the healing following surgery (von Arx, Hänni et al. 2007). In a retrospective study evaluating healing outcomes and their relationship with bone defect dimensions across 215 surgerized teeth, von Arx found a number of parameters associated with healing, including the depth of the bony crypt, the distance from the facial bone plate to the canal, and the overall volume of the crypt. Most importantly, however, he found through logistic

regression that the width of the access window was the significant factor; healed cases had an average width (referred to as length in the paper) of 7.04mm while non-healed cases were 8.60mm.

In light of these findings, it is not surprising that a goal of endodontic microsurgery is to minimize the area of the osteotomy access to improve chances of healing (Kim and Kratchman 2006). This can be particularly difficult for cases in which the periradicular lesion has not perforated the cortical plate, as well as for cases in which the depth of the apex from the cortical plate is greater, necessitating a larger cortical window in order to locate the apex. For example, while the buccal surface of the root 3mm coronal to the apex of mandibular first premolars has been found to be an average of 1.69mm from the cortex, the same location on the mesial root of mandibular first molars is slightly deeper at 1.90mm and the mesial root of mandibular second molars is much deeper at 5.23mm (Uğur Aydın and Göller Bulut 2019).

Another difficulty in endodontic surgery involves the proximity of the root apex to vital structures, such as the inferior alveolar nerve (Suebnukarn, Rhienmora et al. 2012). Locating and resecting the apex of the target tooth could never result in a successful surgery if a structure such as this were damaged during the attempt. As such, the advent and use of cone-beam computed tomography (CBCT) becomes another critical piece of technology that can assist the practitioner in avoiding these structures (Anderson, Wealleans et al. 2018). Many times, standard two-dimensional conventional radiographs are unable to accurately reflect the three-dimensional relationships between the tooth and surrounding structures, and the use of CBCT to establish those relationships becomes necessary (Patel, Durack et al. 2015).

While the spatial information provided by CBCT is a significant benefit to the operator, it is of no use if the operator is unable to translate that into the surgical procedure itself. A subsequent

technology that developed first in the placement of implants is static guidance, in which a stent is fabricated that guides the drill to the appropriate location in the bone. The information acquired by a pre-operative CBCT is used to plan the implant virtually to avoid critical structures and to locate the implant in the ideal location. A stent is designed around that virtual placement. It is subsequently printed or milled, giving the operator the ability to significantly improve the accuracy of placement (Tahmaseb, Wismeijer et al. 2014).

As the technology was shown to be successful in implant placement, it became used in non-surgical endodontics as well. The technique has been reported to be highly accurate when used for access cavity preparation in both a pre-clinical setting (Zehnder, Connert et al. 2016) as well as a clinical setting (Krastl, Zehnder et al. 2016, van der Meer, Vissink et al. 2016). Most of these studies have shown that an access can be achieved that has a deviation of less than 2° from a virtually planned ideal, with an apical bur location of less than 0.5mm from ideal.

A natural evolution from guided non-surgical endodontics is the use of static guidance in endodontic microsurgery. Preclinical results have shown a high degree of accuracy when using 3D printed guides. In one of the first studies, the investigators were able to achieve guided accesses ending <1mm from the apex in 88% of samples, while only 20% of freehand accesses were able to achieve the same precision (Pinsky, Champleboux et al. 2007). A subsequent preclinical study in a cadaver model showed that freehand apical access was only considered clinically successful (i.e. direct access to the apex) in 11/24 samples, while the use of a 3D-printed static guide resulted in success in 24/24 samples (Ackerman, Aguilera et al. 2019). That study reported that the average deviation from ideal was only 1.74mm when using the guide, while the freehand group deviated an average of 2.64mm from ideal.

To date, there have only been a few case reports of static guidance being used in clinical endodontic microsurgery (Strbac, Schnappauf et al. 2017, Ahn, Kim et al. 2018, Giacomino, Ray et al. 2018, Ye, Zhao et al. 2018). All studies reported clinical success, with reduced chair time, minimized osteotomies, precise localization of the apex, and avoidance of adjacent critical anatomy.

There are currently a number of systems available for the practitioner to choose from, including both the aforementioned static guidance as well as dynamic guidance (Tahmaseb, Wismeijer et al. 2014). The first dynamic navigation system for implant placement was introduced in 2000 (Panchal, Mahmood et al. 2019), and the first studies on the accuracy of dynamic navigation in the placement of implants were published in 2001 (Jung, Schneider et al. 2009).

One such system is the X-Guide Surgical Navigation System by X-Nav Technologies (Lansdale, PA, USA) (Figure 1). This system utilizes an array of cameras in the operatory to triangulate the location of both a dental handpiece and a marker rigidly attached to adjacent dentition in the patient's mouth. After taking a CBCT image of the patient's jaw, the operator virtually plans an implant. During the procedure, the cameras track the location of the handpiece and provide visual feedback to the operator regarding the location & angulation of the bur tip on a computer monitor in the operatory.

Figure 1: X-Guide hardware and workflow (courtesy X-Nav Technologies)

Just as with static guidance, dynamic guidance has also been shown to be significantly more accurate than freehand implant placement, with one study showing mean angular deviation of 2.97° using dynamic navigation as compared to a deviation of 6.50° for freehand placement (Emery, Merritt et al. 2016). A number of other studies have also shown that dynamic guidance is very accurate in the placement of implants (Block, Emery et al. 2017, Panchal, Mahmood et al. 2019). However, there have only been limited case reports published showing the use of this technology in endodontic microsurgery. One case report highlights the effectiveness of this technology in that successful apical surgery (near-complete healing in six months) was performed by a pre-doctoral dental student with no previous experience in endodontic microsurgery (Gambarini, Galli et al. 2019).

Despite this successful case report, there have been no pre-clinical studies published that directly compare the effectiveness of dynamic guidance technology as compared to a freehand technique

in the preparation of osteotomies. Therefore, the purpose of this in-vitro study was to compare dynamically guided osteotomy to freehand osteotomy in terms of parameters critical to the success of endodontic microsurgery, including mean access-window area, osteotomy volume, osteotomy depth past target root, root resection length and apical bevel.

Materials & Methods

Thirty-six human mandibular posterior teeth were collected and distributed such that twelve dental stone casts could be poured with one premolar (1P), one first molar (1M) and one second molar (2M) each; six casts included teeth on the right side, and six casts included teeth on the left side. The target roots were the single-rooted premolar and the mesial roots of the molars. Prior to casting the models, the roots of the teeth were dipped in melted wax to simulate a periodontal ligament both clinically and radiographically. Initial CBCT images of the casts were acquired by a Planmeca ProMid3D ProFace (Planmeca USA, Inc., Hoffman Estates, IL, USA) and trimmed such that the thickness of the stone at a point 3mm coronal to the apex was within one standard deviation of the average thickness of buccal bone as reported in a previous anatomical study (Uğur Aydın and Göller Bulut 2019). Those measurements were as follows: first premolar (1.63 ± 0.98mm), first molar mesial root (1.91 ± 1.31mm) and second molar mesial root (5.23 ± 2.30mm).

The casts were randomly divided into two groups using a random number generator in Microsoft Excel. Each group consisted of three casts with study teeth on the right side and three casts with study teeth on the left side. In one group (Group DG), the X-Nav System was used to plan (Figure 2) and execute (Figure 3) an initial osteotomy and apex localization of the target root using a #8 round carbide bur, followed by opening the osteotomy conventionally using tapered diamond burs such that an effective retropreparation could be performed. In the other group (Group FH) the osteotomies and root-end resections were performed freehand by an experienced faculty endodontist.

To plan the osteotomies in Group DG, the X-Guide X-Clip was mounted onto the contralateral mandibular posterior teeth in accordance with the manufacturer's instructions, and a final treatment image was acquired. Those images were imported into X-Guide software where osteotomies were planned for root-end resection of the apices of the target roots. Those osteotomies were planned with a 2.2mm #8 round bur in order to locate and begin to resect the target root at 3mm from the apex. The osteotomies were also planned such that an approximately 10° B-L bevel resulted along the resected surface.

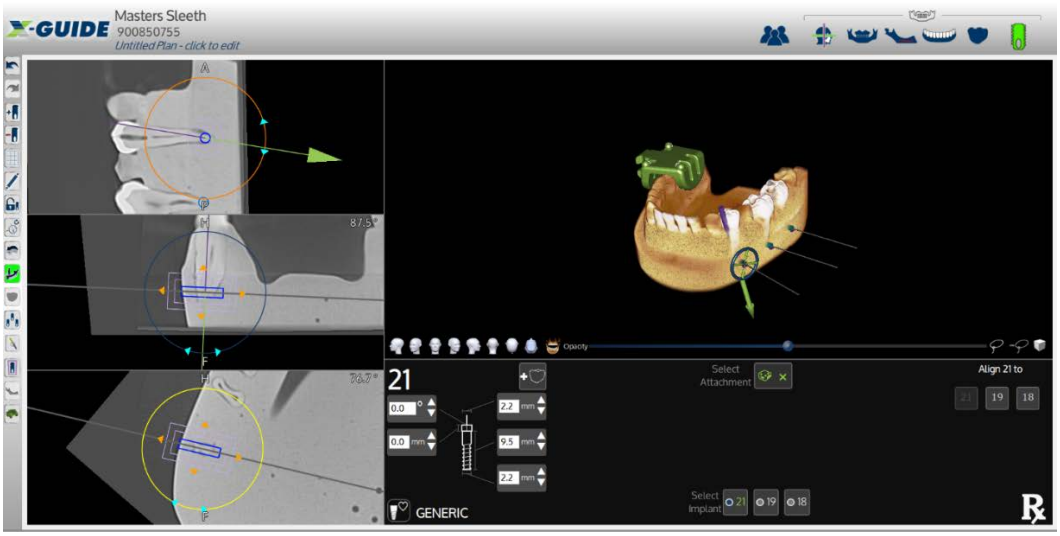

Figure 2: Screenshot of typical access plan in X-Guide software.

The goal of the preparations in each group was that a conservative osteotomy was performed such that a 3mm resection could be executed, the resected portion of the root could be fully inspected using a micromirror and that a 3mm ultrasonic retropreparation tip could access the root canal (retropreparations were initiated, however, were not fully executed because the selected teeth had not been previously endodontically treated).

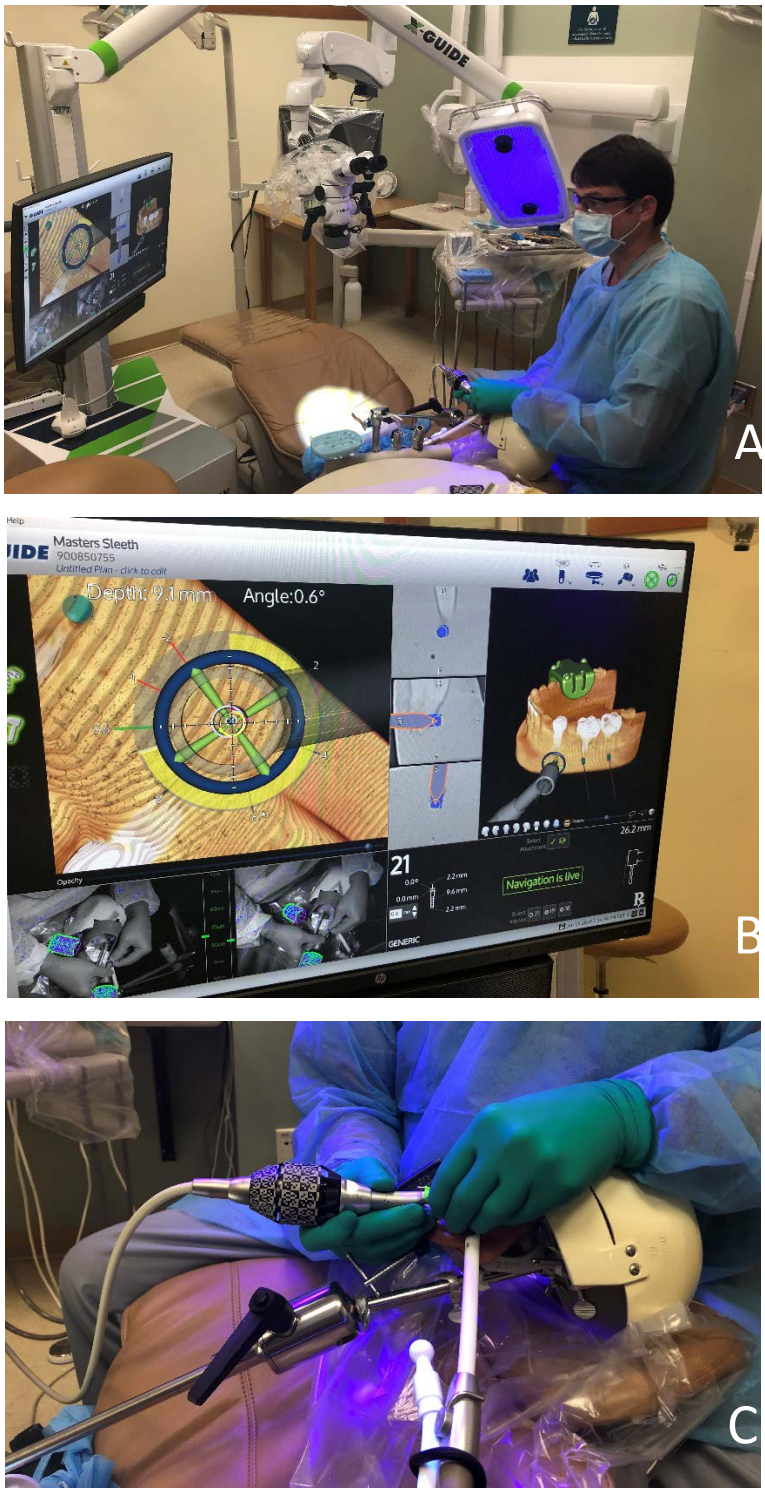

Figure 3: Intra-operative photos taken during guided access procedure. Photograph A is an operatory view showing camera system & display screen; note the eyes of the operator focusing on the screen. Photograph B shows the guidance display tracking the aim/angulation/depth of the handpiece, the location of the bur in three planes and a three-dimensional rendering of the procedure. Photograph C shows a hand-level view of the procedure being executed.

Following the clinical procedure, final CBCT images were taken with the same Planmeca CBCT machine. Integral functions in Romexis software (Planmeca USA, Inc., Hoffman Estates, IL, USA) were used to view the images and assess the volume of the osteotomies, the area of the osteotomy window (both using the free region grow tool [Figure 4]) and the length & bevel of the resection. A mid-treatment CBCT image was also taken in Group DG to quantify whether the target root was successfully located.

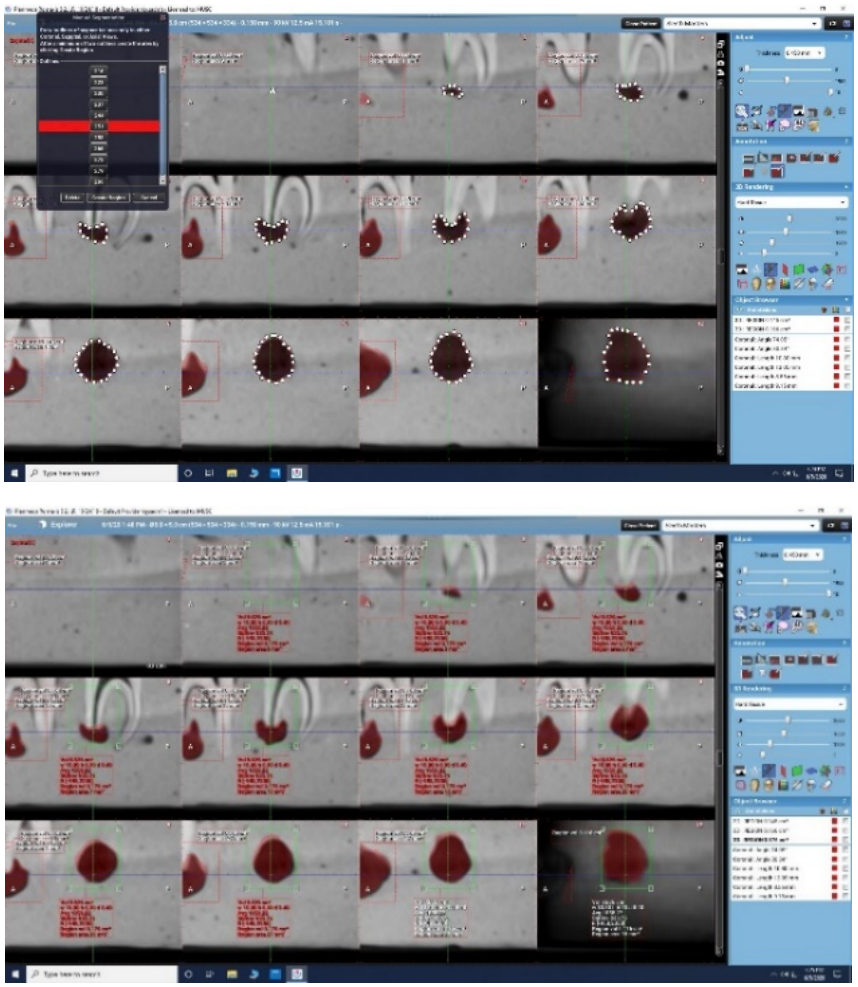

Figure 4: Romexis free region grow tool used to calculate osteotomy volume. The image on the top shows the outlines of the region being identified in successive 1mm planes. The image on the bottom shows the data output once the outlines were completed.

T-tests were used to compare groups for Window, Volume, Depth, Bevel and Resection; a Bonferroni adjustment was made to account for the fact that there were multiple outcomes from the same tooth. Analysis of variance was used to compare tooth subgroups (1P, 1M & 2M) for each outcome.

Results

Significant differences were found between Group FH & Group DG in the osteotomy window area, volume, and depth past the target root (Table 1). The mean area of the osteotomy window across all tooth types for Group FH was 37.56mm^2 (±5.02) and for Group DG was only 18.28mm^2 (±7.04) ($p<0.0001$). Mean volume of the osteotomy for Group FH was 0.23cm^3 (±0.05) and for Group DG was only 0.13cm^3 (±0.06) ($p<0.0001$). There were no significant differences between the two groups in overall depth of the crypt, however there were significant differences in depth of the crypt past the target root, with Group FH extending 2.88mm (±1.12) past the target root on average, while the guided group only extended 1.12mm (±0.33) past ($p<0.0001$).

With respect to the roots, additional significant differences were found in the amount of bevel achieved as well as for the amount of root that was resected. In terms of bevel, Group FH had a significantly greater bevel than Group DG, with values of 11.8° (±3.99) and 6.24° (±2.51) respectively ($p<0.0001$). Surprisingly, significantly less root was resected in the freehand group (1.75mm ± 0.81) than in the guided group (3.78mm ± 0.69) ($p<0.0001$), despite a bulk of the root being exposed during the procedure prior to the resection.

Assessment by tooth subgroup revealed no significantly different results. Overall data is presented in Appendix 1.

Table 1: Mean overall values for the investigated parameters by primary group (freehand v guided). Statistically significant differences ($p<0.0001$) were found for Window, Volume, Depth Past Root, Bevel and Resection.

Group	n	**Window (mm^2)**	Std Dev	Min.	Max	p
FH	18	37.6	5.02	29	47	p<0.0001
DG	15	18.28	7.04	10	23	

Group	n	**Volume (cm^3)**	Std Dev	Min.	Max	p
FH	18	0.23	0.05	0.145	0.307	p<0.0001
DG	15	0.13	0.06	0.071	0.195	

Group	n	**Depth Past Root (mm)**	Std Dev	Min.	Max	p
FH	18	2.88	1.12	1.05	4.65	p<0.0001
DG	15	1.12	0.33	0.60	1.35	

Group	n	**Bevel (°)**	Std Dev	Min.	Max	p
FH	18	11.80	3.99	2.73	19.65	p<0.0001
DG	15	6.24	2.51	0.00	9.09	

Group	n	**Resection (mm)**	Std Dev	Min.	Max	p
FH	18	1.75	0.81	0.60	3.45	p<0.0001
DG	15	3.78	0.69	2.06	4.95	

Mid-treatment CBCT images taken in Group DG revealed that 100% of the target roots were located and resected as planned, without impacting adjacent critical anatomy such as non-target roots (Figure 5). However, the conservative nature of the osteotomies in the guided group did result in one resection being clinically unacceptable, with a fin of root structure being left in place after expanding the initial guided osteotomy.

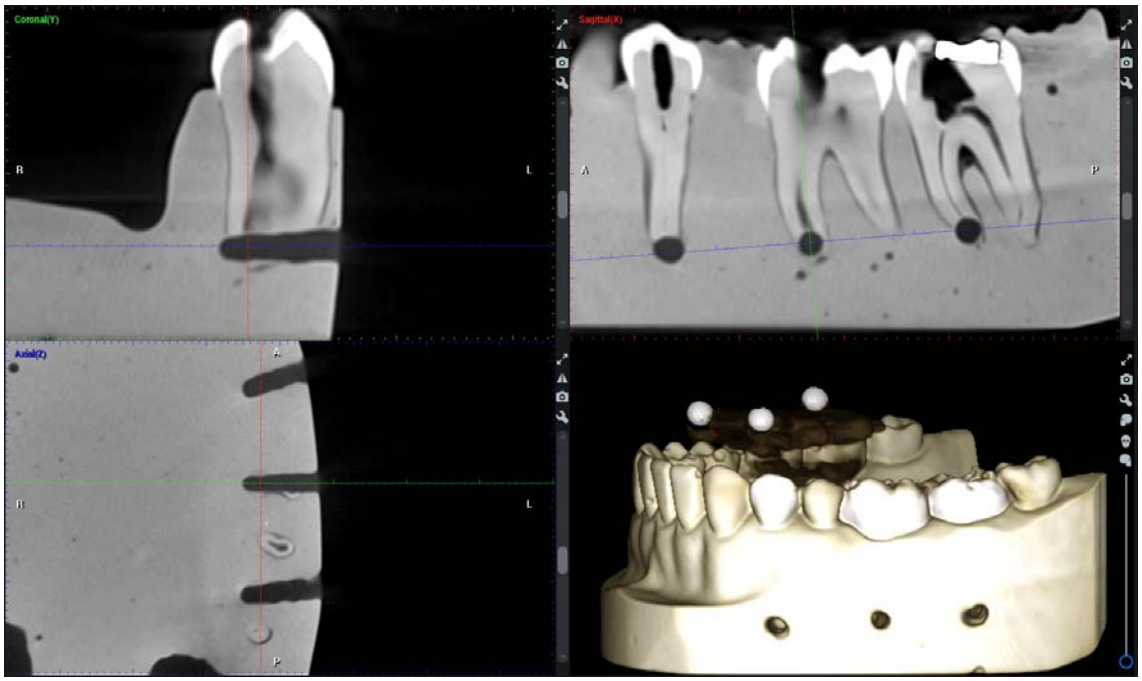

Figure 5: Typical intra-operative CBCT image showing the ability of dynamic guidance to localize the target apex.

The initial plan for Group DG was to use a 4mm trephine bur to complete the osteotomy and resection using a single bur, however it became clear in the first study cast that the technique could not be used because the stone and dehydrated dentin were too hard for the trephine bur to cut; this resulted in one study cast having to be discarded & not incorporated into the statistical analysis.

Discussion

Results of the present study showed that dynamic guidance can confer upon the operator the ability to prepare more conservative osteotomies with a high degree of accuracy (Figures 6 & 7). The average osteotomy window area using dynamic guidance was less than half of the area created with the freehand technique. In addition to the study by von Arx highlighting improved healing with smaller osteotomies, Jansson also found that successful cases tended towards having

smaller osteotomy sizes (5.9mm diameter) than uncertain or unsuccessful cases (7.5mm & 7.0mm, respectively) after one year, although the result was not significant (Jansson, Sandstedt et al. 1997). Calculating the diameter from the average area of the windows in the freehand group in the present study shows that the average diameter is nearly 7mm, which places these osteotomies among the less successful categories in the Jansson study. On the other hand, the average diameter in the guided group was only 4.5mm which would fall well below the 5.9mm threshold identified by Jansson for cases that saw better healing outcomes. As such, it can be expected that the smaller window provided via dynamic guidance could result in better healing outcomes.

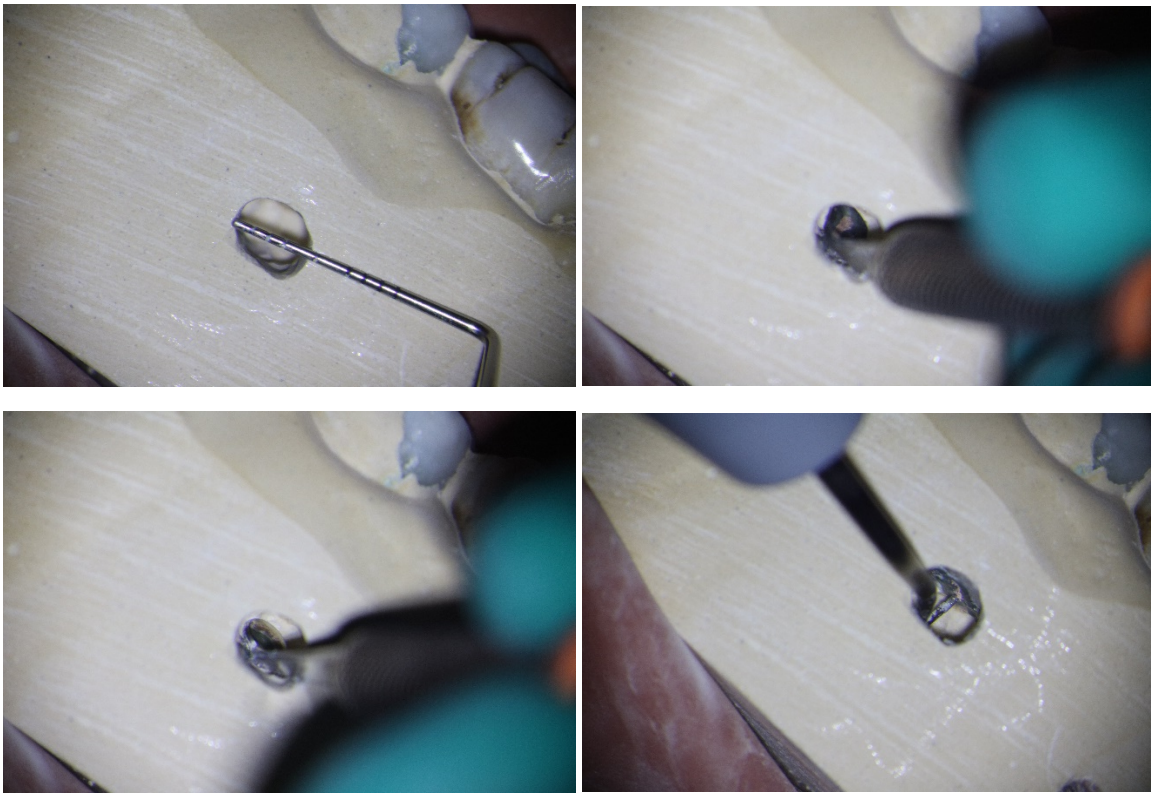

Figure 6: Intra-operative photographs of mandibular second molar osteotomy following dynamically guided access & refinement. Clockwise from top left: periodontal probe showing 4x5mm osteotomy, micromirror providing inspection of canal space; micromirror providing inspection of lingual extent of resected root surface, 3mm ultrasonic retropreparation tip at canal.

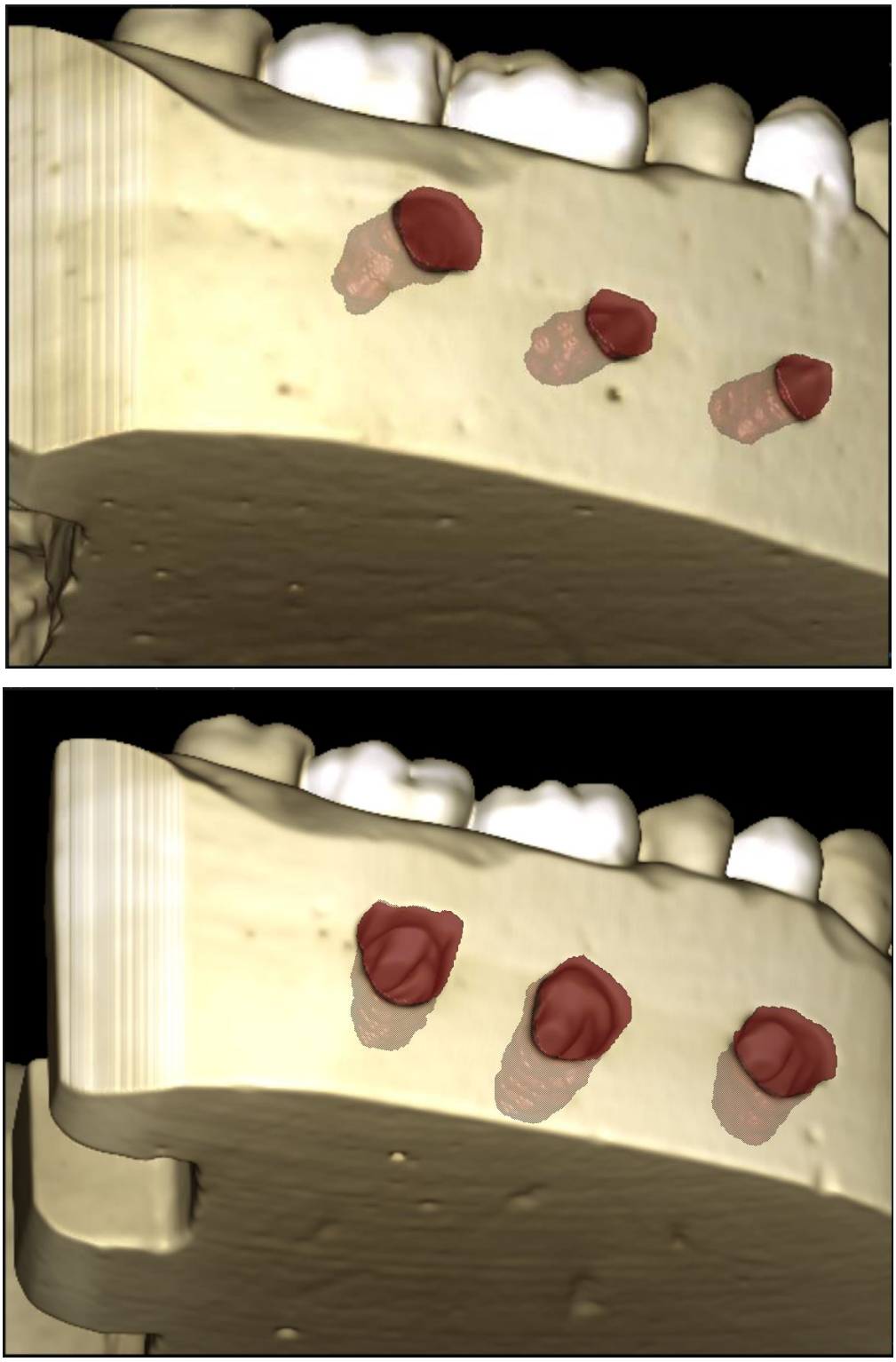

Figure 7: Three-dimensional renderings of the osteotomies created using dynamic guidance (top) and freehand (bottom). Note the reduced size of both the access window and overall volume provided by dynamic guidance versus freehand.

In addition to these studies, the Toronto Study also identified that the size of the surgical crypt is a predictor of success. That study showed that surgeries with crypts <10mm in diameter had an 80% success rate, while those with diameters >10mm had only a 53% success rate (Barone, Dao et al. 2010). In the present study, although the crypts in the freehand group did not exceed 10mm, they were significantly larger than the guided osteotomies and could therefore be expected to result in reduced success.

Yet another study highlighting the effect of osseous defect size on healing was conducted by Murphy et al., in which it was found that osseous healing occurs at a rate of approximately 3.2mm^2/month (Murphy, Kaugars et al. 1991). While this study focused on healing after non-surgical endodontic therapy, it provides a healing rate that can generally be applied to post-surgical healing. When applied to the results of the present study, the freehand osteotomies would heal in an average of 11.75 months, while it would only take 4.9 months for healing to take place in the guided group.

Another significant difference between the two groups was that the guided group was able to provide a significantly shallower osteotomy depth (past the root) than the freehand group. The ability of dynamic guidance to define the overall depth of the osteotomy in relation to the target apex reduces the risk of the surgeon extending the removal of bone excessively and unnecessarily past the target root. This will both reduce the overall volume of the osteotomy as well as reduce the chance of the surgeon impacting critical structures deep to the target root.

Dynamic guidance was also able to facilitate significantly shallower bevels (6.24°) than the freehand technique (11.80°). There is debate regarding the amount of bevel that is ideal. Historically, a 0° bevel has been the goal. According to Gilheany & Figdor, greater bevel angles require greater depth of retroprep/fill to seal effectively (Gilheany, Figdor et al. 1994). Bevels

closer to 0° are more able to be sealed well during retrofill, thus improving chances of healing. However, in the present study, the amount of bevel achieved with both techniques was clinically acceptable.

With respect to the amount of root resection achieved by the two groups, the freehand group failed to achieve the necessary 3mm of root resection in 16/18 teeth, thereby leaving potentially infectious apical ramifications that could result in surgical failure for most teeth (Kim and Kratchman 2006). On the other hand, the dynamically guided group achieved the 3mm standard in all but one tooth. However, these resections did exceed the 3mm standard by an average of 0.71mm. This has the potential of reducing the crown-root ratio to a point at which the surgerized tooth becomes unstable. This was likely because the initial localization using the dynamic guidance was planned to resect at 3mm, and subsequent opening of that osteotomy resulted in additional root structure being removed unnecessarily. Care should therefore be taken to either plan the initial osteotomy more apically, or to subsequently expand the osteotomy more apically following initial localization.

Assessment of tooth subgroups revealed no significant differences within teeth across all parameters. This shows that dynamic guidance can provide similar improvement over freehand results whether it is employed on first premolars or second molars.

In the guided group, there was one instance of a clinically unacceptable resection in which a fin of root structure was not removed, leaving an uneven resection surface. This was likely the result of the conservative nature of the osteotomies in this group, which made adequate inspection of the crypt difficult. When preparing these conservative osteotomies, the operator should ensure that either a significant effort is made to closely inspect the crypt and resected root surface, to

open the osteotomy further to facilitate such inspection if it is not initially possible, and to take intra-operative radiographs (which was not done in the present study).

The accuracy of the dimensional measurements obtained through the Planmeca software has been established in previous studies. Sonmez et al. compared dimensional measurements obtained by the Planmeca Romexis software to direct measurements of external resorptive defects and found that the measurements obtained through the CBCT software are clinically acceptable, with a difference of 0.008mm for linear measurements and only 0.062mm^3 for volumetric measurements (Sönmez, Koç et al. 2018). Therefore, it can be assumed that the measurements obtained in this study are clinically accurate.

A major subjective observation made during this study was that the X-Guide software is intuitive, easy to use and can be learned in short-order. Taking a pre-operative CBCT image prior to endodontic microsurgery is quickly becoming the standard of care, if it is not already, and simply placing the X-Clip when taking that image takes almost no additional time. Once that image is taken, importing the image into the X-Guide software takes only seconds, the access path can be planned in minutes and calibration of the system in the operatory also only takes minutes. This was the primary investigator's first exposure to the system, and he was able to plan 18 osteotomies in under an hour. One significant drawback to the implementation of this system is the capital investment required to obtain the system itself, the exact magnitude of which is not a subject of the present paper & which needs to be addressed by the manufacturer.

While there are no comparable studies on the use of dynamic guidance in endodontic microsurgery available to which the present results can be related, a similarly high level of accuracy has been seen in implant studies using dynamic guidance. Block found that dynamic navigation significantly improved the location accuracy of implant placement, with the apical

portion of the implant being located an average of 1.29mm from the ideal position, while freehand placement resulted in the apex of the implant being located 2.27mm from ideal (Block, Emery et al. 2017).

Although this study did highlight many potential benefits of using dynamic guidance in endodontic microsurgery, it also had several significant limitations. First and foremost, the study was executed on stone models, so many of the obstacles encountered in live surgery such as blood, saliva and flap management were not present. The fact that there were no apical lesions present in the study models perhaps made it more difficult for the operator in the freehand group to more easily locate the target root, potentially resulting in a larger osteotomy & window than could be achievable when a lesion is present.

The time needed to perform these procedures could not be quantified because of the desire to capture a mid-treatment CBCT image in the dynamic guidance group. Subjectively, it seemed that while accessing the target root using guided access could be achieved in less than a minute, refining an extremely conservative access did take noticeably more time than was needed in the freehand group. Future studies should be designed such that time can be analyzed as well.

The initial experimental design was to evaluate guided access using a trephine bur such that the osteotomy and resection could be executed with a single bur. While this technique has been used successfully in a clinical setting (Giacomino, Ray et al. 2018, Ye, Zhao et al. 2018), it was found that the stone model and dehydrated dentin was too hard for the trephine bur to successfully cut. In fact, studies have found that normally hydrated dentin has a hardness of 0.3 +/- 0.05 GPa, while the hardness of dehydrated dentin is 0.92 +/- 0.12 GPa (Guidoni, Denkmayr et al. 2006), a three-fold increase. Future studies should take this difference into account in experimental designs, perhaps by performing the osteotomy/resection immediately after casting a hydrated tooth into

the stone model, or even by eliminating the natural tooth altogether and using 3-D printed models. The use of 3-D models would have the added benefit of standardizing the conditions under which the comparison between freehand and guided surgery is performed, especially with respect to the anatomy of the target roots and the depth of the osteotomy required.

Future studies should also incorporate teeth (either natural or 3-D printed) on which a full surgical procedure (retroprep/fill) can be completed to ensure that the conservative osteotomy provided by dynamic guidance is a condition under which the microsurgery can be clinically executable.

Conclusion:

The results of this study show that implementing dynamic guidance in endodontic microsurgery has the potential to significantly reduce the osteotomy window area and osteotomy volume as compared to freehand surgery, which can subsequently result in improved healing. It can also help ensure that critical structures such as adjacent non-target roots and the mandibular canal are avoided while attempting to locate the target root.

References

Ackerman, S., F. C. Aguilera, J. M. Buie, G. N. Glickman, M. Umorin, Q. Wang and P. Jalali (2019). "Accuracy of 3-dimensional–printed Endodontic Surgical Guide: A Human Cadaver Study." Journal of Endodontics **45**(5): 615-618.

Ahn, S.-Y., N.-H. Kim, S. Kim, B. Karabucak and E. Kim (2018). "Computer-aided Design/Computer-aided Manufacturing–guided Endodontic Surgery: Guided Osteotomy and Apex Localization in a Mandibular Molar with a Thick Buccal Bone Plate." Journal of Endodontics **44**(4): 665-670.

Anderson, J., J. Wealleans and J. Ray (2018). "Endodontic applications of 3D printing." International Endodontic Journal **51**(9): 1005-1018.

Barone, C., T. T. Dao, B. B. Basrani, N. Wang and S. Friedman (2010). "Treatment Outcome in Endodontics: The Toronto Study—Phases 3, 4, and 5: Apical Surgery." Journal of Endodontics **36**(1): 28-35.

Block, M. S., R. W. Emery, D. R. Cullum and A. Sheikh (2017). "Implant Placement Is More Accurate Using Dynamic Navigation." Journal of Oral and Maxillofacial Surgery **75**(7): 1377-1386.

Emery, R. W., S. A. Merritt, K. Lank and J. D. Gibbs (2016). "Accuracy of Dynamic Navigation for Dental Implant Placement–Model-Based Evaluation." Journal of Oral Implantology **42**(5): 399-405.

Gambarini, G., M. Galli, L. V. Stefanelli, D. Di Nardo, A. Morese, M. Seracchiani, F. De Angelis, S. Di Carlo and L. Testarelli (2019). "Endodontic Microsurgery Using Dynamic Navigation System: A Case Report." Journal of Endodontics **45**(11): 1397-1402.e1396.

Giacomino, C. M., J. J. Ray and J. A. Wealleans (2018). "Targeted Endodontic Microsurgery: A Novel Approach to Anatomically Challenging Scenarios Using 3-dimensional–printed Guides and Trephine Burs—A Report of 3 Cases." Journal of Endodontics **44**(4): 671-677.

Gilheany, P. A., D. Figdor and M. J. Tyas (1994). "Apical dentin permeability and microleakage associated with root end resection and retrograde filling." Journal of Endodontics **20**(1): 22-26.

Guidoni, G., J. Denkmayr, T. Schöberl and I. Jäger (2006). "Nanoindentation in teeth: influence of experimental conditions on local mechanical properties." Philosophical Magazine **86**(33-35): 5705-5714.

Hargreaves (2016). Cohen's Pathways of the Pulp, Elsevier.

Jansson, L., P. Sandstedt, A.-C. Låftman and A. Skoglund (1997). "Relationship between apical and marginal healing in periradicular surgery." Oral Surgery, Oral Medicine, Oral Pathology, Oral Radiology, and Endodontology **83**(5): 596-601.

Jung, R. E., D. Schneider, C. H. F. Hammerle, J. Ganeles, D. Wismeijer, M. Zwahlen and A. Tahmaseb (2009). "Computer technology applications in surgical implant dentistry: A systematic review." International Journal of Oral and Maxillofacial Implants **24**: 92-109.

Kim, S. and S. Kratchman (2006). "Modern Endodontic Surgery Concepts and Practice: A Review." Journal of Endodontics **32**(7): 601-623.

Krastl, G., M. S. Zehnder, T. Connert, R. Weiger and S. Kühl (2016). "Guided Endodontics: a novel treatment approach for teeth with pulp canal calcification and apical pathology." Dental Traumatology **32**(3): 240-246.

Murphy, W. K., G. E. Kaugars, W. K. Collett and R. N. Dodds (1991). "Healing of periapical radiolucencies after nonsurgical endodontic therapy." Oral Surgery, Oral Medicine, Oral Pathology **71**(5): 620-624.

Panchal, N., L. Mahmood, A. Retana and R. Emery (2019). "Dynamic Navigation for Dental Implant Surgery." Oral and Maxillofacial Surgery Clinics of North America **31**(4): 539-547.

Patel, S., C. Durack, F. Abella, H. Shemesh, M. Roig and K. Lemberg (2015). "Cone beam computed tomography in Endodontics – a review." International Endodontic Journal **48**(1): 3-15.
Pinsky, H. M., G. Champleboux and D. P. Sarment (2007). "Periapical Surgery Using CAD/CAM Guidance: Preclinical Results." Journal of Endodontics **33**(2): 148-151.
Setzer, F. C., S. B. Shah, M. R. Kohli, B. Karabucak and S. Kim (2010). "Outcome of Endodontic Surgery: A Meta-analysis of the Literature—Part 1: Comparison of Traditional Root-end Surgery and Endodontic Microsurgery." Journal of Endodontics **36**(11): 1757-1765.
Song, M., S. G. Kim, S.-J. Lee, B. Kim and E. Kim (2013). "Prognostic Factors of Clinical Outcomes in Endodontic Microsurgery: A Prospective Study." Journal of Endodontics **39**(12): 1491-1497.
Sönmez, G., C. Koç and K. Kamburoğlu (2018). "Accuracy of linear and volumetric measurements of artificial ERR cavities by using CBCT images obtained at 4 different voxel sizes and measured by using 4 different software: an ex vivo research." Dento maxillo facial radiology **47**(8): 20170325-20170325.
Strbac, G. D., A. Schnappauf, K. Giannis, A. Moritz and C. Ulm (2017). "Guided Modern Endodontic Surgery: A Novel Approach for Guided Osteotomy and Root Resection." Journal of Endodontics **43**(3): 496-501.
Suebnukarn, S., P. Rhienmora and P. Haddawy (2012). "The use of cone-beam computed tomography and virtual reality simulation for pre-surgical practice in endodontic microsurgery." International Endodontic Journal **45**(7): 627-632.
Tahmaseb, A., D. Wismeijer, W. Coucke and W. Derksen (2014). "Computer technology applications in surgical implant dentistry: a systematic review." The International journal of oral & maxillofacial implants **29**(Suppl): 25-42.
Uğur Aydın, Z. and D. Göller Bulut (2019). "Relationship between the anatomic structures and mandibular posterior teeth for endodontic surgery in a Turkish population: a cone-beam computed tomographic analysis." Clinical Oral Investigations **23**(9): 3637-3644.
van der Meer, W. J., A. Vissink, Y. L. Ng and K. Gulabivala (2016). "3D Computer aided treatment planning in endodontics." Journal of Dentistry **45**: 67-72.
von Arx, T., S. Hänni and S. S. Jensen (2007). "Correlation of Bone Defect Dimensions with Healing Outcome One Year after Apical Surgery." Journal of Endodontics **33**(9): 1044-1048.
Ye, S., S. Zhao, W. Wang, Q. Jiang and X. Yang (2018). "A novel method for periapical microsurgery with the aid of 3D technology: a case report." BMC Oral Health **18**(1): 85.
Zehnder, M. S., T. Connert, R. Weiger, G. Krastl and S. Kühl (2016). "Guided endodontics: accuracy of a novel method for guided access cavity preparation and root canal location." International Endodontic Journal **49**(10): 966-972.

Appendix 1: Overall Data

Group	Cast	Tooth	Window (mm^2)	Volume (cm^3)	Bevel (°)	Resection (mm)	Depth Past Root (mm)
FH	1	1P	39	0.179	12.26	1.65	4.50
FH	1	1M	40	0.282	11.31	1.94	4.50
FH	1	2M	39	0.226	11.69	1.79	2.11
FH	2	1P	32	0.227	13.39	2.16	4.65
FH	2	1M	38	0.256	10.71	2.4	3.00
FH	2	2M	47	0.296	11.31	3.45	1.05
FH	5	1P	39	0.242	16.40	1.35	3.75
FH	5	1M	40	0.307	16.75	0.60	2.70
FH	5	2M	43	0.245	12.53	3.12	1.65
FH	8	1P	31	0.168	7.13	1.05	3.15
FH	8	1M	32	0.200	2.73	1.05	2.40
FH	8	2M	32	0.221	8.75	0.75	2.85
FH	9	1P	29	0.166	19.65	2.56	4.35
FH	9	1M	45	0.294	10.49	1.05	1.65
FH	9	2M	36	0.263	8.13	0.90	3.00
FH	12	1P	36	0.145	9.16	1.66	2.10
FH	12	1M	42	0.166	15.95	2.40	3.00
FH	12	2M	36	0.176	14.03	1.65	1.50
DG	3	1P	14	0.076	2.73	3.90	1.50
DG	3	1M	15	0.117	4.90	3.44	1.00
DG	3	2M	18	0.195	4.67	4.39	0.60
DG	6	1P	12	0.068	7.85	3.90	1.00
DG	6	1M	14	0.101	5.19	3.91	1.05
DG	6	2M	23	0.186	0.00	4.95	1.35
DG	7	1P	13	0.080	8.97	2.06	1.50
DG	7	1M	12	0.095	7.12	3.12	1.50
DG	7	2M	12	0.101	4.40	3.46	1.00
DG	10	1P	10	0.071	6.12	4.21	1.50
DG	10	1M	16	0.113	5.86	4.65	1.50
DG	10	2M	17	0.131	11.00	3.90	0.75
DG	11	1P	17	0.086	9.09	3.73	0.75
DG	11	1M	22	0.124	7.59	3.00	1.00
DG	11	2M	20	0.122	6.34	3.01	0.75